First and second order in magnetization effects in optical second-harmonic generation from a trilayer magnetic structure

I. A. Kolmychek,[1,*] V. L. Krutyanskiy,[1] T. V. Murzina,[1] M. V. Sapozhnikov,[2,3] E. A. Karashtin,[2,3] V. V. Rogov,[2] and A. A. Fraerman[2,3]

[1]*Department of Physics, Moscow State University, 119991 Moscow, Russia*
[2]*Institute for Physics of Microstructures RAS, GSP-105, Nizhny Novgorod 603950, Russia*
[3]*University of Nizhny Novgorod, 23 Prospekt Gagarina, Nizhny Novgorod 603950, Russia*
**Corresponding author: irisha@shg.ru*

Received September 26, 2014; revised December 24, 2014; accepted December 25, 2014; posted January 6, 2015 (Doc. ID 223882); published January 22, 2015

Linear and nonlinear optical properties of a thin planar $CoFe/Al_2O_3/CoFe$ structure for different angles of incidence of the fundamental radiation are studied by means of the magneto-optical Kerr effect and magnetization-induced second-harmonic generation (SHG). The composition of this multilayered structure supports the appearance of the antiferromagnetic state, which leads to nonreciprocal optical effects and is discussed in terms of the magnetic toroid moment. We show that in accordance with the phenomenological description, SHG magnetic hysteresis loops for a linearly polarized pump beam are determined by linear in magnetization M components of the SHG polarization, while for a circularly polarized pump such a description necessarily involves both linear and quadratic in M components of the nonlinear polarization. Symmetry analysis of the magnetization-induced SHG supports the differences between the cases of linear and circular polarization of the incident radiation observed in the experiment, as well as a partial suppression of first in magnetization SHG contributions. Relative values of the linear and quadratic in magnetization components of the SHG polarization are estimated for the trilayer structure and for a reference homogeneous ferromagnetic film.

OCIS codes: (190.4400) Nonlinear optics, materials; (160.3820) Magneto-optical materials; (160.4236) Nanomaterials.

http://dx.doi.org/10.1364/JOSAB.32.000331

1. INTRODUCTION

The development of technological methods allows us to provide the control over the magnetization distribution on the nanometer scale and opens up additional opportunities to introduce new magnetic and transport effects in artificial nanomaterials. First of all, one should mention here the spin-dependent tunneling and giant magnetoresistance [1–5], magnetorefractive effect (MRE) [6], magnetic switching behavior, shape, and magnetoelastic anisotropy [7], etc. In turn, these modify the magneto-optical (MO) response of the structures, giving rise to peculiarities in the values and magnetic field dependencies of the MO Faraday and Kerr effects [6,8,9], which may be used as remote and sensitive characterization methods.

Among a variety of optical methods, a distinguished place belongs to optical second-harmonic generation (SHG), which is known as an effective diagnostic tool of surfaces, interfaces, and nanostructures [10,11]. This is due to a unique sensitivity of the SHG process to any kind of symmetry breaking, as the second-order nonlinear susceptibility vanishes in media with inversion symmetry in the electric dipole approximation. In the case of magnetic nanostructures, additional magnetization-induced components of the nonlinear susceptibility tensor appear in the regions of the symmetry breaking, thus allowing for a direct investigation of interfacial magnetic properties in layered magnetic nanostructures [12–14].

It was demonstrated that the SHG technique allows us to investigate different types of magnetic ordering that cannot be detected by the linear MO Kerr effect (MOKE) [15–19]. In particular, SHG induced by the magnetic toroid moment [20,21] in bulky dielectrics has been demonstrated [22,23].

Still, there is a definite gap in the research of this kind concerning the studies of the role of inhomogeneous distribution of magnetization in the linear and nonlinear optical response of artificial planar magnetic nanostructures. Recently we studied the main features of the linear and nonlinear optical response of planar (2D) lattices of nanoparticles with vortex magnetic ordering [24,25] and showed that the observed peculiarities of the SHG hysteresis loops are attributed to the existence of the magnetic toroid moment. Here, we consider the most simple structure exhibiting the macroscopic toroid moment and formed by two magnetic layers separated by a thin nonmagnetic spacer. For an antiparallel alignment of in-plane magnetic moments of the adjacent layers, the system reveals the toroid moment oriented in the plane of the structure. The aim of this paper is to study experimentally the appearance of linear and nonlinear optical effects that are of the first or the second order in magnetization **M**. We demonstrate that the use of a circularly polarized fundamental beam may help to pick out the second order in **M** effects in the SHG polarization and provide further information on the magnetization reversal, on the exchange splitting in multilayer magnetic structures, etc. The high order in magnetization effects in SHG was studied earlier in homogeneous ferromagnetic film [26], but to the best of our knowledge, such a study of the

structures possessing the toroid moment has not been performed until now.

The paper is organized as follows: Section 2 combines general aspects of the MO and nonlinear MO responses of magnetic films; Section 3 describes the studied samples and the main experimental methods used in this work. The experimental investigations of nonlinear MO responses of a single ferromagnetic film and of a trilayer structure along with the linear effects for the latter are described in Section 4. The discussion of the obtained results and comparison with the model description are summarized in Section 5, followed by conclusions in Section 6. Symmetry analysis of the second-order susceptibility is performed in Appendix A.

2. PHENOMENOLOGICAL DESCRIPTION OF THE OPTICAL RESPONSE OF MAGNETIC MONOLAYER AND TRILAYER STRUCTURES

The optical response of a medium is described by the polarization **P** induced by the electric field of the incident light wave $\mathbf{E}(\omega)$, which can be expanded in its powers, so that in the electric dipole approximation **P** takes the form

$$\mathbf{P} = \mathbf{P}_\omega + \mathbf{P}_{2\omega} + \ldots; \mathbf{P}_\omega \propto \hat{\chi}^{(1)}\mathbf{E}_\omega; \mathbf{P}_{2\omega} \propto \hat{\chi}^{(2)}\mathbf{E}_\omega\mathbf{E}_\omega + \ldots, \quad (1)$$

where the first- and second-order polarization terms are considered, $\hat{\chi}^{(1)}$ and $\hat{\chi}^{(2)}$ being the first- and the second-order susceptibility tensors, respectively; the subscripts ω and 2ω denote the frequency of the fundamental and second-harmonic fields. The tensor $\hat{\chi}^{(1)}$ exists in media of any type of symmetry, while $\hat{\chi}^{(2)}$ vanishes in centrosymmetric ones, as is the case of metals and amorphous oxides [27]. However, $\hat{\chi}^{(2)}$ as an even-order susceptibility tensor appears in spatial regions with broken inversion symmetry, and thus the SHG sources in the case of multilayer structures are commonly attributed to the infinitely thin layer at the interface between the adjacent layers.

Magnetization leads to the appearance of additional symmetry operations, which give rise to magnetization-induced components of the susceptibility tensors, which can be considered by the following expression for the linear polarization:

$$\mathbf{P}_\omega \propto \{\hat{\chi}^{(1)\mathrm{cr}} + \hat{\chi}^{(1)\mathrm{odd}}(M) + \hat{\chi}^{(1)\mathrm{ev}}(M)\}\mathbf{E}_\omega. \quad (2)$$

The second order in M linear effect $\hat{\chi}^{(1)\mathrm{ev}}$ is known as the MRE [28]. It is observed in the IR spectral range and is usually not greater than 1% with respect to $\hat{\chi}^{(1)\mathrm{cr}}$. Similarly, for the SHG polarization [16],

$$\mathbf{P}_{2\omega} \propto \{\hat{\chi}^{(2)\mathrm{cr}} + \hat{\chi}^{(2)\mathrm{odd}}(M) + \hat{\chi}^{(2)\mathrm{ev}}(M)\}\mathbf{E}_\omega\mathbf{E}_\omega, \quad (3)$$

where the superscript cr stands for the crystallographic (nonmagnetic) contributions to the corresponding fields and the superscripts odd and ev denote the susceptibility components that are odd (i.e., change their sign as $M \to -M$) and even in M, respectively [16]. This approach treats the magnetization as a parameter and allows us to compare the relative susceptibility terms in Eqs. (2) and (3). In other definitions, one can express these components as $\chi_{ijk}^{(2)\mathrm{odd}}(M) \propto \chi_{ijkl}^{(2)}M_l$, $\chi_{ijk}^{(2)\mathrm{ev}}(M) \propto \chi_{ijklm}^{(2)}M_lM_m$ [18,29]. The role of the symmetry of $\hat{\chi}^{(2)\mathrm{odd}}$ and $\hat{\chi}^{(2)\mathrm{ev}}$ in the SHG response will be discussed in more detail below (see Appendix A). It is commonly accepted that $|\chi_{ijk}^{(2)\mathrm{odd}}| \gg |\chi_{ijk}^{(2)\mathrm{ev}}|$, and thus second order in M effects can be hardly observed in the experiment.

In order to describe the SHG from a heterostructure, one has to consider the contributions from the nonlinear sources at all the interfaces that are accessed by light. The simplest case is a trilayer structure consisting of two identical in-plane isotropic magnetic layers (labeled by the subscripts I and II) with different coercivity separated by a thin nonmagnetic layer. In that case, the SHG process at the interfaces with air and with the substrate is described by Eq. (3) with the substitution of M_I and M_{II}, respectively, while the input of the interface between the magnetic films (denoted by the subscripts I and II) separated by a nonmagnetic spacer requires special treatment. For a nanometer-thin spacer the second-order polarization from this interface can be nonzero due to (i) opposite orientations of the magnetic moments of the layers, (ii) the optical field gradient along the normal to the structure, and (iii) different properties of the upward and downward interfaces. For the odd in M contribution of the trilayer we have in the dipole approximation

$$P_{i,2\omega}^{\mathrm{odd}} \propto \ldots + \chi_{ijklm}n_jM_{I,k}E_{l,\omega}E_{m,\omega} - \chi_{ijklm}n_jM_{II,k}E_{l\omega}E_{m,\omega} + \ldots, \quad (4)$$

where **n** is a unit vector directed from film I to film II. For the sake of simplicity hereafter, we omitted the superscript (2) for all the susceptibilities. Considering isotropic and homogeneous magnetic films, Eq. (4) in the vector form looks like

$$\mathbf{P}_{2\omega}^{\mathrm{odd}} \propto \ldots + \hat{\chi}_{T1}(\mathbf{T}\mathbf{E}_\omega)\mathbf{E}_\omega + \hat{\chi}_{T2}\mathbf{T}(\mathbf{E}_\omega)^2 + \ldots, \quad (5)$$

where $\mathbf{T} = [(\mathbf{M}_I - \mathbf{M}_{II}) \times \mathbf{n}]$ is the magnetic toroid moment of the system and $\hat{\chi}_{T1}$ and $\hat{\chi}_{T2}$ are the corresponding susceptibility tensors.

A similar approach can be used for the description of the SHG polarization terms that are *second order* (even) in magnetization, the most interesting being the contributions that are proportional to the product $\mathbf{M}_I \cdot \mathbf{M}_{II}$. Phenomenologically, the corresponding SHG polarization takes the form

$$P_{i,2\omega}^{\mathrm{ev}} \propto \ldots + \chi_{ijklmn}n_jM_{I,k}M_{II,l}E_{m,\omega}E_{n,\omega} + \tilde{\chi}_{ijklmn}M_{I,j}M_{II,k}E_{l,\omega}\nabla_mE_{n,\omega} + \ldots, \quad (6)$$

where the first term describes nonequivalence of the upward and downward magnetic interfaces. The second one appears if we do not restrict ourselves to the dipole approximation; it is responsible for the spatial dispersion of $\mathbf{E}_\omega$ along the normal to the trilayer.

It is clear from Eqs. (5) and (6) that when changing the direction of **n**, we change the sign of the magnetization-induced effect, similar to what is described in [30] for the linear-optical case.

The mechanisms underlying the interactions between the magnetic layers may be different, but it is expected that the main role belongs to the exchange interaction of electrons from the adjacent layers. These terms of the SHG polarization should satisfy the principle of the "exchange symmetry" [31], i.e., they should be invariant with respect to a coherent **M** rotation. Taking into account these requirements, Eq. (6) can be rewritten as

$$\mathbf{P}_{2\omega}^{\mathrm{ev}} \propto \ldots + \delta\mathbf{n}(\mathbf{M}_I \cdot \mathbf{M}_{II})(E_\omega^2) + \gamma(\mathbf{M}_I \cdot \mathbf{M}_{II})(\mathbf{n} \cdot \mathbf{E}_\omega)\mathbf{E}_\omega + \tilde{\delta}(\mathbf{M}_I \cdot \mathbf{M}_{II})\nabla(E_\omega^2) + \tilde{\gamma}(\mathbf{M}_I \cdot \mathbf{M}_{II})\mathbf{E}_\omega(\nabla\mathbf{E}_\omega). \quad (7)$$

Note that it is the scalar product $(\mathbf{M}_I \cdot \mathbf{M}_{II})$ that determines the magnetic field dependence of the resistivity in multilayer structures as well as of the MRE [6]. Experimental studies of the nonlinear optical effects described by Eqs. (6) and (7) are discussed in Section 4.B.

In a more compact form, SHG polarization for a magnetic trilayer structure can be expressed as

$$\mathbf{P}_{2\omega} \propto [\hat{\chi}_I^{\mathrm{cr}} + \hat{\chi}_I^{\mathrm{odd}} + \hat{\chi}_I^{\mathrm{ev}} + \hat{\chi}_{II}^{\mathrm{cr}} + \hat{\chi}_{II}^{\mathrm{odd}} + \hat{\chi}_{II}^{\mathrm{ev}} + \hat{\chi}_{I+II}^{\mathrm{ev}}]\mathbf{E}_\omega\mathbf{E}_\omega, \quad (8)$$

where we introduced the effective susceptibility tensors for each layer.

Finally, let us consider the phenomenological analysis of the linear MO response of a trilayer. In that case the reciprocity theorem should be valid, so that the differential cross section of the diffracted light intensity σ satisfies the equality $\sigma(\mathbf{k}, \mathbf{k}', \mathbf{M}(\mathbf{r})) = \sigma(-\mathbf{k}', -\mathbf{k}, -\mathbf{M}(\mathbf{r}))$, where $\mathbf{k}$ and $\mathbf{k}'$ are the wave vectors of the incident and diffracted beams and $\mathbf{M}(\mathbf{r})$ is the spatial distribution of magnetization [32,33]. Thus the possible intensity MO effects can be described by the following expression:

$$I = I_0 + \alpha((\mathbf{k} + \mathbf{k}') \cdot [\mathbf{n} \times \langle\mathbf{M}\rangle]) + \beta([\mathbf{k} \times \mathbf{k}'] \cdot \langle\mathbf{M}\rangle) + \gamma((\mathbf{k} + \mathbf{k}') \cdot \mathbf{T}), \quad (9)$$

where I_0 is the independent of M intensity component, $\langle\mathbf{M}\rangle$ is the magnetization averaged over the trilayer structure and α, β, γ are phenomenological coefficients. The transversal MOKE is described by the vector product $\beta([\mathbf{k} \times \mathbf{k}'] \cdot \langle\mathbf{M}\rangle)$ [third term in Eq. (9)], which vanishes in the transmission geometry for symmetric structures [30]. The last term in Eq. (9) appears only for structures with spatial inhomogeneity of the magnetization distribution.

3. SAMPLES AND EXPERIMENTAL SETUP

A. Samples

Ferromagnetic trilayer structures were made by magnetron sputtering of thin $Co_{0.6}Fe_{0.4}$ films on the surface of SiO_2 plates. In order to reduce the coercivity of the first layer, it was deposited on a Ni_3Fe sublayer. We used a 2 nm thick dielectric interlayer to separate the ferromagnetic films. This was an Al layer oxidized in the oxygen plasma. This method of obtaining continuous Al_2O_3 films is well known and time tested [34]. Then the second magnetic field was deposited. The pressure of Ar during the deposition was $4 * 10^{-3}$ Torr, and the film's growth rate was 1 nm/s. The thicknesses of the first and the second CoFe layers were 10 and 20 nm, respectively. The structure of a trilayer sample is shown schematically in Fig. 1(a). The presence of a soft permalloy sublayer on the substrate made the neighbor CoFe layer softer compared to the upper magnetic layer, so that the antiferromagnetic state could be formed. As a reference sample, a homogeneous 60 nm thick Co film deposited on a glass substrate was used.

B. Linear Magneto-Optical Setup

The linear MOKE was measured using the p-polarized radiation of a He–Ne laser at a 628 nm wavelength falling on the sample from the film side, as shown in Fig. 1(a), at a 45° angle of incidence. The samples were placed in a longitudinal magnetic field $\mathbf{H}$, and the dependence of the angle of the polarization plane rotation of the reflected beam on H was measured.

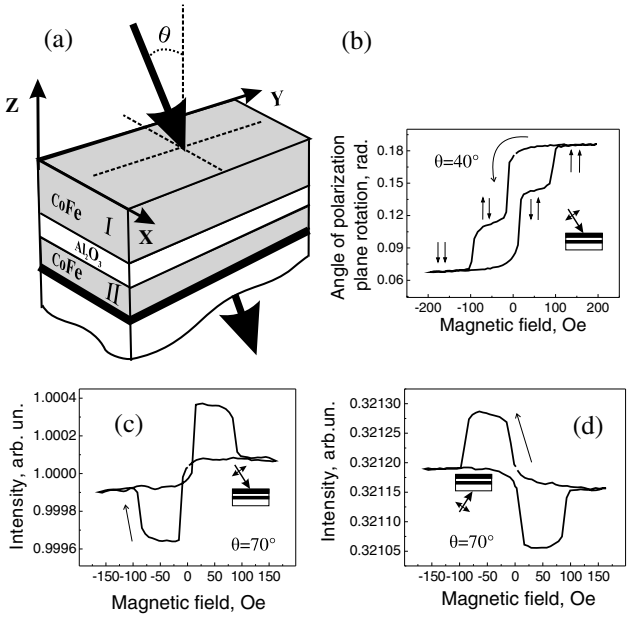

Fig. 1. (a) Schematic view of the $CoFe/Al_2O_3/CoFe$ structure and geometry of the nonlinear optical experiment, (b) the dependence of longitudinal MOKE on the applied magnetic field (the beam lies in the XOZ plane), (c) the dependence of the intensity of the transmitted light for the transversal magnetization geometry and for a 70° angle of incidence (fundamental beam falls from the film side), (d) the dependence of the intensity of the transmitted light for the transversal magnetization geometry and for a 70° angle of incidence (fundamental beam falls from the substrate side).

The reflectance and transmittance of the trilayers were measured for both p and s polarizations of the incident light. The angle of incidence was varied in the range of 5°–85° measured from the surface normal.

C. Nonlinear Magneto-Optical Experiments

For the SHG experiments linearly (p) or *circularly* polarized radiation of a Ti:sapphire laser was used at a wavelength of 780 nm, a pulse duration of 80 fs, a repetition frequency of 80 MHz, and a mean power of 100 mW. The pump radiation was focused on the sample into a spot approximately 100 μm in diameter, so the peak power was about 2.5 kW/cm^2. The angle of incidence of the fundamental beam was varied in the interval from 5° to 50°. p-polarized SHG radiation, transmitted through the film, was spectrally selected by BG39 Schott color filters and detected by a photomultiplier operating in the photon counting mode. During the magnetic measurements, the sample was placed between the poles of the electromagnet that formed the transversal magnetic field.

4. EXPERIMENTAL RESULTS

A. Linear Magneto-Optical Kerr Effect

A typical MOKE hysteresis loop of a trilayer measured for a 45° angle of incidence is shown in Fig. 1(b). It reveals two steps that are attributed to the contributions of the two magnetic layers, with the coercive forces being $H_{c_I} = 93$ Oe and $H_{c_{II}} = 14$ Oe into the polarization plane rotation. Thus, four

magnetic states of the structure can be distinguished that are characterized by the parallel or antiparallel orientation of the magnetic moments of the neighbor layers, shown schematically by arrows.

Figure 1(c) shows the measured dependence of the transmittance on the external magnetic field for a 70° angle of incidence and for the transversal MOKE geometry. Significant transmittance modulation can be seen for the H values that correspond to antiferromagnetic trilayer state, while for the ferromagnetic state the relative variation of the transmitted intensity is less pronounced for the chosen measurement geometry. The presented experimental data demonstrate that, first, the intensity of the transmitted light I_ω is odd in both average magnetization and the toroid moment, as $I_\omega(M) \neq I_\omega(-M)$ and $I_\omega(T) \neq I_\omega(-T)$, as is described by Eq. (9). Second, we demonstrate that reversal of the direction of the incident beam propagation (i.e., whether it illuminates the trilayer film first and then passes to the substrate or vice versa) changes the sign of the intensity modulation $\delta I_\omega = I_\omega(H) - I_\omega(H = 0)$, as we change the direction of the vector **n**. This is a manifestation of the nonreciprocal nature of this effect, described by the second term in Eq. (9) [30].

Finally, the MO effect in transmission is observed for the p-polarized light only; no magnetization-dependent effects were detected for the s-polarized light. This is consistent with the symmetry of the transversal MO effect in transmission, which may be observed in a layered structure with nonequivalent interfaces [30].

Importantly, the observed linear MO effects are well described by the Fresnel formulas for the reflected and transmitted light that do not take into account any interactions between the magnetic layers [31].

B. Nonlinear Optical Studies

Nonlinear optical studies of the reflected SHG from magnetic homogeneous films and from trilayer structures have shown that the quadratic signal is specular and p-polarized; this is typical for a coherent nonlinear optical signal. Coherence of the SHG radiation indicates that the surface and interfaces inside the films are planar and smooth [35].

As the first step, we studied the magnetic field dependence of the SHG intensity for a thick homogeneous magnetic film. The idea was to figure out the main features of the SHG magnetic hysteresis loops obtained for the linearly and circularly polarized fundamental radiation.

1. Homogeneous Magnetic Film

Figures 2(a)–2(c) show the magnetic hysteresis loops of the SHG intensity for a uniform Co film measured for different angles of incidence of the p-polarized fundamental beam ($\theta = 20°$, 30°, and 40°). The shape of these dependencies is typical for the SHG response from ferromagnetic surfaces [36]. Approximations of these SHG dependencies by Eq. (3) are shown in the figure by solid lines. It was found that the second order (even) in M components of the nonlinear polarization are negligibly small compared to χ^{cr} and χ^{odd}. This is in agreement with the common approach to the description of the magnetization-induced SHG effects.

For the approximation we used the proportionality $\chi^{\mathrm{odd}} \propto M$ and described $M(H)$ dependence by the function $M(H) \propto A \tan(\gamma(H - H_c))$, H_c being the coercive force.

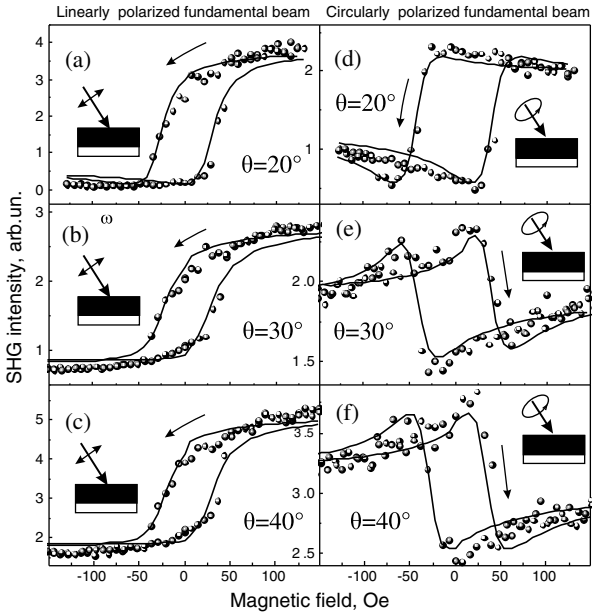

Fig. 2. SHG intensity hysteresis loops measured for a uniform Co film (a)–(c) for the *linear* polarization of the fundamental radiation and (d)–(f) for the *circular* polarization; the angle of incidence is (a), (d) 20°; (b), (e) 30°; and (c), (f) 40°.

Based on the data from Fig. 2 for the saturating H values, the SHG magnetic contrast was calculated as [11]

$$\rho_{2\omega} = \frac{I_{2\omega}(H) - I_{2\omega}(-H)}{I_{2\omega}(H) + I_{2\omega}(-H)}, \tag{10}$$

where $I_{2\omega}(H)$ and $I_{2\omega}(-H)$ are the SHG intensities for the opposite directions of the (saturating) transversal magnetic field. It was found that $\rho_{2\omega}$ is about 92% for $\theta = 20°$, 56% for $\theta = 30°$, and 52% for $\theta = 40°$. Detailed measurements have shown that $\rho_{2\omega}$ is positive for all available θ values and decreases with increasing θ. Such behavior is in agreement with the expressions $\chi^{\mathrm{cr}}_{pp} \propto \sin\theta$ and $\chi^{\mathrm{odd}}_{pp} \propto \cos\theta$ discussed in Appendix A.

Figures 2(d)–2(f) show analogous SHG hysteresis loops measured for the *circularly* polarized incident beam. It can be seen that the shape of the dependencies differs greatly from the case of linear polarization. Moreover, the SHG magnetic contrast changes its sign as the angle of incidence increases; we find that $\rho_{2\omega} = 32\%$ for $\theta = 20°$, while it is –1% and –7% for $\theta = 30°$ and 40°, respectively.

Thus the following differences between the SHG dependencies obtained for the linearly and circularly polarized fundamental light can be noted: (i) $\rho_{2\omega}$ values are smaller for the circularly polarized fundamental beam compared to the case of p polarization for the same angles of incidence; and (ii) $\rho_{2\omega}$ changes its sign at definite θ values, which cannot be achieved for the linearly polarized fundamental beam. As is shown in Appendix A, these features can be explained when considering the expressions for the effective SHG susceptibility that determine the SHG process for the linearly and circularly polarized fundamental beams.

Importantly, both renamed peculiarities of the SHG hysteresis loops indicate that second order (even) in M contributions are more pronounced for the circularly polarized fundamental beam. Indeed, we found that the approximation of the SHG magnetic hysteresis loops requires consideration

of the χ^{ev} terms. Thus the experimental dependencies shown in Fig. 2 were approximated by the expressions $I^{cp}_{2\omega}(H) \propto |\chi^{cr}_{cp} + \chi^{odd}_{cp} e^{i\phi} + \chi^{ev}_{cp} e^{i\psi}|^2$, χ^{cr}_{cp}, χ^{odd}_{cp}, and χ^{ev}_{cp}, and the phases ϕ and ψ between the corresponding fields are fitting parameters, $M(H) \propto A \tan(\gamma(H - H_c))$, where H_c and γ were taken from the previous approximation (for a linearly polarized pump). The subscript cp is used here to indicate that we consider the *p*-polarized SHG field excited by the circularly polarized fundamental radiation. The following relative values of odd and even in M susceptibility components [with respect to the crystallographic (nonmagnetic) ones] were obtained: $|\chi^{odd}_{cp}/\chi^{cr}_{cp}| = 0.60 \pm 0.07$ and $|\chi^{ev}_{cp}/\chi^{cr}_{cp}| = 0.25 \pm 0.03$. In other words, even in M contributions are observable in the quadratic response when using circularly polarized fundamental radiation and are found to be of the same order of magnitude as odd ones.

2. Magnetic Trilayer Films

Magnetic hysteresis loops of the transmitted SHG intensity for a trilayer $CoFe/Al_2O_3/CoFe$ film are shown in Fig. 3. Linear [Figs. 3(a)–3(c)] or circular [Figs. 3(d)–3(f)] polarization of the fundamental radiation was used to illuminate the sample. It can be seen that for a small angle $\theta = 5°$ the shape of the hysteresis loop is far from being trivial [see Figs. 3(a)–3(d)]. First of all, it reveals wide "wings" for the magnetic field values that correspond to the antiferromagnetic state, and nearly zero SHG magnetic contrast for the saturating H values. Moreover, the SHG curve intersects itself at $H = 0$, thus formally giving a zero width of the SHG hysteresis loop. This indicates that magnetization-induced (odd and even) SHG contributions prevail over nonmagnetic ones for small θ values. This is as expected, taking into account that nonmagnetic SHG tends to zero for $\theta \to 0$ for isotropic surfaces.

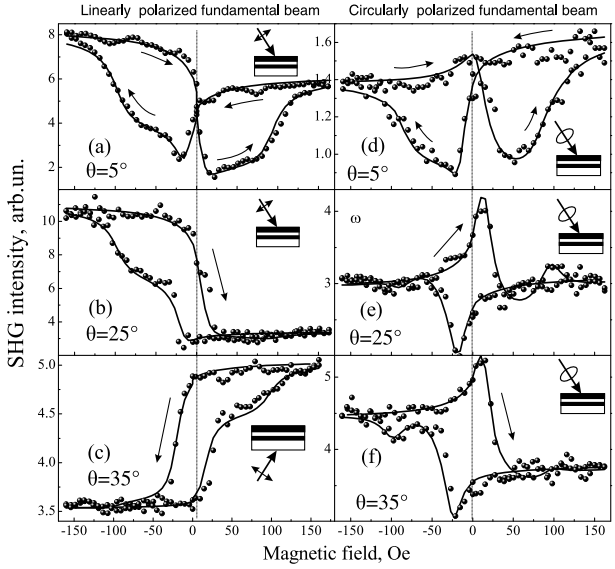

Fig. 3. SHG intensity hysteresis loops measured for a $CoFe/Al_2O_3/CoFe$ trilayer (a)–(c) for the *linear* polarization of the fundamental radiation and (d)–(f) for the *circular* polarization; the angle of incidence is (a), (d) 5°; (b), (e) 25°; and (c), (f) 35°. The fundamental radiation falls from the trilayer side [parts (a), (b), (d)–(f)] or from the substrate [part (c)], as is shown schematically in the insets. Experimental data in parts (a)–(c) were fitted by the function in Eq. (11) and in parts (d)–(f) by the function in Eq. (12).

SHG hysteresis loops were measured for the angle of incidence up to $\theta = 50°$; a typical dependence is shown in Fig. 3(b). Two steps in the SHG hysteresis loops correspond to the coercivity of the two ferromagnetic layers, $H_{c_I} = 93$ Oe and $H_{c_{II}} = 14$ Oe, similar to those observed in linear MO curves (Fig. 1). Figure 3(c) shows the SHG hysteresis loop for the studied structure as the linearly polarized fundamental radiation illuminated the sample from the substrate side, i.e., from the opposite side of the sample as compared to the dependence shown in Fig. 3(b). This is shown schematically on the insets in the figure. It can be seen that Figs. 3(b) and 3(c) are qualitatively mirrorlike images of each other, the signs of the SHG magnetic contrast changes also being opposite in these two cases. This was expected based on analogy with the linear MO transversal effect as well as with the symmetry consideration for the magnetization-induced SHG [30,37].

The SHG magnetic field dependencies presented in Figs. 3(a)–3(c) were approximated by the function

$$I^{pp}_{2\omega}(H) \propto (|\chi^{cr}_{pp} + \chi^{odd}_{pp,I} e^{i\phi_I} + \chi^{odd}_{pp,II} e^{i\phi_{II}}|^2), \tag{11}$$

where ϕ_I and ϕ_{II} are the relative phases of the odd in M components with respect to the crystallographic SHG field. Here, we omitted the second order in M contributions, which turned out to be zero within the approximation error, similar to the case of a homogeneous magnetic film. The modulus of the ratio $\chi^{odd}_{pp}/\chi^{cr}_{pp}$ for the two layers and for the saturating magnetic field are summarized in Table 1. One can see that odd magnetic contributions from both layers decrease with increasing θ for a *p*-polarized pump beam in accordance with the phenomenological treatment (see Appendix A).

The second-order susceptibility induced by the magnetic toroid moment was estimated as $|\chi_T| \propto |\chi^{odd}_I| - |\chi^{odd}_{II}|$, where we took into account the fact that the magnetic moments of the two layers are parallel to the plane of the trilayer. The corresponding results (in arbitrary units) are shown in the fourth column of Table 1. It can be seen that the T-induced susceptibility component tends to decrease as θ increases. This is reasonable if we take into account the fact that the toroid moment of the system is also lying in the plane of the structure, and thus the relative value of the T-induced SHG contribution should also decrease with the rising angle of incidence.

Let us now consider the case of the *circularly* polarized incident beam. Figures 3(d)–3(f) show the SHG hysteresis loops measured for the angles of incidence $\theta = 5°$, 25°, and 35°. Similar to the case of a homogeneous Co film, SHG

Table 1. Fitting Parameters Obtained from the SHG Hysteresis Loops of a Trilayer Magnetic Structure (*p*-Polarized Fundamental Radiation, Film Side)

θ	$\lvert\chi^{odd}_{pp,I}/\chi^{cr}_{pp}\rvert$	$\lvert\chi^{odd}_{pp,II}/\chi^{cr}_{pp}\rvert$	$\lvert\chi_T/\chi^{cr}_{pp}\rvert$
5°	0.30	0.65	0.35
20	0.14	0.42	0.28
25°	0.11	0.34	0.23
35°	0.08	0.19	0.11
40°	0.05	0.21	0.16
50°	0.04	0.19	0.15

Table 2. Fitting Parameters Obtained from the Hysteresis SHG Loops in Trilayer Film (*Circularly*-Polarized Fundamental Radiation, Film Side)

θ	$\left\lvert\frac{\chi^{\mathrm{odd}}_{\mathrm{cp},I}}{\chi^{\mathrm{cr}}_{\mathrm{cp}}}\right\rvert$	$\left\lvert\frac{\chi^{\mathrm{odd}}_{\mathrm{cp},II}}{\chi^{\mathrm{cr}}_{\mathrm{cp}}}\right\rvert$	$\left\lvert\frac{\chi^{\mathrm{ev}}_{\mathrm{cp},I}}{\chi^{\mathrm{cr}}_{\mathrm{cp}}}\right\rvert$	$\left\lvert\frac{\chi^{\mathrm{ev}}_{\mathrm{cp},II}}{\chi^{\mathrm{cr}}_{\mathrm{cp}}}\right\rvert$	$\left\lvert\frac{\chi^{\mathrm{ev}}_{\mathrm{cp},I+II}}{\chi^{\mathrm{cr}}_{\mathrm{cp}}}\right\rvert$
5°	0.07	0.63	0.02	0.29	0.11
20°	0.21	0.43	0.08	0.16	0.18
25°	0.11	0.16	0.10	0.10	0.23
30°	0.01	0.21	0.02	0.05	0.05
35°	0.24	0.37	0.07	0.11	0.14
50°	0.09	0.14	0.06	0.09	0.21

magnetic contrast in that case approaches zero and changes the sign as $\theta \to 25°$, as can be seen in Fig. 3(e). The analysis performed in Appendix A testifies that this is expected for the circular polarization of the fundamental beam, unlike the case of a linearly polarized pump.

The graphs shown in Figs. 3(d)–3(f) were approximated by the function

$$I^{\mathrm{cp}}_{2\omega}(H) \propto |\chi^{\mathrm{cr}}_{\mathrm{cp}} + \chi^{\mathrm{odd}}_{\mathrm{cp},I} e^{i\phi_I} + \chi^{\mathrm{odd}}_{\mathrm{cp},II} e^{i\phi_{II}} + \chi^{\mathrm{ev}}_{\mathrm{cp},I} e^{i\psi_I} + \chi^{\mathrm{ev}}_{\mathrm{cp},II} e^{i\psi_{II}} + \chi^{\mathrm{ev}}_{\mathrm{cp},I+II} e^{i\phi_{I+II}}|^2. \quad (12)$$

The dependencies $M_i(H)$, $i = I, II$ were assumed to be the same as in Eq. (11). The fitting parameters obtained from the approximation are summarized in Table 2. Again, similar to the case of a homogeneous cobalt film, even in M components for both magnetic films in the trilayer are large enough and are comparable to odd ones.

Moreover, it stems from the approximation that the SHG term described by $\chi^{\mathrm{ev}}_{I+II}$ appears when we use the circularly polarized fundamental beam. The symmetry of the corresponding terms fits the restrictions imposed by the exchange interaction of the magnetic layers in the structure. It is clear from Table 2 that the amplitudes of the "exchange" terms exceed those of the other even SHG terms at definite θ values and thus may be the most pronounced in the magnetization-induced SHG effects.

5. DISCUSSION

The main result to be discussed is the appearance of the second order in magnetization contributions to the nonlinear polarization of the studied structures and the consequences of this effect.

As was noted above, the effective odd and even in magnetization susceptibility terms are of the same order of magnitude for circularly polarized incident light only, which turns out to be a distinguishing property of the circular pump polarization.

The main mechanism underlying this effect is a relative suppression of the effective odd in M susceptibility components, which is attained for the circularly polarized fundamental radiation; this is discussed in detail in Appendix A. Namely, an additional second-order susceptibility component $\chi^{\mathrm{odd}}_{xyy}$ appears in that case in the expression for the SHG polarization, its sign being opposite to the other summands in the expression for the $\chi^{\mathrm{odd}}_{\mathrm{cp}}$. Therefore, this component can compensate the others for a definite angle of incidence, similar to what was observed in the experiment, leading to nearly zero SHG magnetic contrast for large enough magnetic field values [see Fig. 3(e)]. Thus the next order in magnetization terms, the

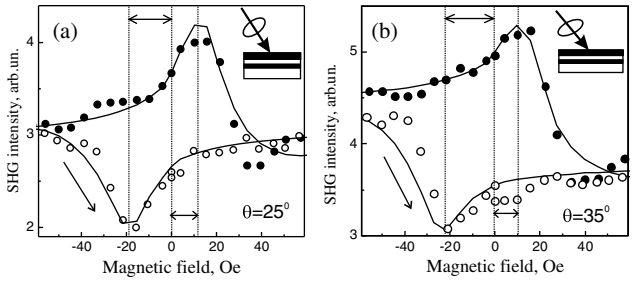

Fig. 4. SHG intensity hysteresis loops in larger scale measured for a $CoFe/Al_2O_3/CoFe$ trilayer film using the circular polarization of the fundamental radiation for (a) $\theta = 25°$ and (b) $\theta = 35°$.

second-order (even) ones, are the main ones to determine the SHG intensity hysteresis loops.

Another interesting effect that was not observed earlier is the appearance of the "exchange" terms that are proportional to the scalar product of the magnetic moments of the two adjacent layers, $P^{\mathrm{ev}}_{I+II} \propto M_I M_{II}$. This stems from the finding in Table 2 that $|\chi^{\mathrm{ev}}_{\mathrm{cp},I+II}|/|\chi^{\mathrm{ev}}_{\mathrm{cp},I}| \geq 2$ and $|\chi^{\mathrm{ev}}_{\mathrm{cp},I+II}|/|\chi^{\mathrm{ev}}_{\mathrm{cp},II}| \geq 1$ for a wide interval of the angle of incidence; this is quite a commensurate even in magnetization effect. Aside from the approximation, the appearance of the P^{ev}_{I+II} contribution can be understood when analyzing the measured SHG hysteresis loops at relatively small values of the magnetic field H, as is shown in more detail in Fig. 4. The difference in the $|H|$ values that correspond to the extrema of the magnetic field dependencies of the SHG intensity is only related to this SHG contribution. We have checked that this difference is not due to the remanent magnetization of the electromagnet (we used a coreless electromagnet).

Regarding results of the approximation, we also saw that this sort of asymmetry of the SHG hysteresis loops vanishes as the term P^{ev}_{I+II} is excluded from the mathematical expression. In that case the mean square approximation error increases significantly.

It is also worth noting that for all angles of incidence susceptibility components for the soft magnetic bottom CoFe layer prevail over the corresponding components of the upper magnetic layer (see Tables 1 and 2). This can be explained by the fact that the interfaces of the bottom magnetic layer are more "asymmetric," as this layer borders on dielectric Al_2O_3 and metal Ni_3Fe, while the upper CoFe layer borders on dielectric materials on both sides.

6. CONCLUSION

To sum up, we have studied linear and nonlinear MO properties of $CoFe/Al_2O_3/CoFe$ structures and of the reference homogeneous Co film. It has been shown that for circular polarization of the fundamental beam, both odd and even in magnetization effects determine the magnetization-induced SHG effect, the values of the corresponding susceptibility components being comparable for a wide interval of the angle of incidence. In contrast, just odd in magnetization terms are sufficient for the description of the SHG hysteresis loops for linearly polarized fundamental radiation. A phenomenological description of the SHG process in a trilayer magnetic structure was presented that considered even in M effects, including those that can be attributed to the exchange interaction between the magnetic layers. The symmetry analysis of the SHG process performed clarified the difference between cir-

cular and linear polarizations of the fundamental radiation in the appearance of the even in M contribution in the SHG intensity modulation. Specifically, we showed that a suppression of odd in magnetization SHG components takes place for the circularly polarized pump, thus making even (second order in **M** effects) more pronounced. Moreover, we emphasized the effect of the exchange interaction of magnetic layers, which cannot be observed by means of linear magneto-optics and magnetization-induced SHG for a linearly polarized pump. The results presented demonstrate the necessity of considering the second order in M effects in the nonlinear optical response for the case of circularly polarized pump radiation.

APPENDIX A

A symmetry analysis of second-harmonic generation from the surface of a magnetized centrosymmetric metal was first performed in [16], where even and odd in magnetization components of the susceptibility tensor were introduced. For the case of thin magnetic films the SHG response is formed by the two interfaces; the second-order susceptibility of each of them contains the components that are independent and odd (linear) and even (second order) in M ($\hat{\chi}^{\mathrm{cr}}$, $\hat{\chi}^{\mathrm{odd}}(M)$, and $\hat{\chi}^{\mathrm{ev}}(M)$, respectively). In what follows we assume that magnetic layer(s) are homogeneous and isotropic, and their magnetic moments are characterized by the dependence $M_i(\mathbf{H})$. Note that in a general case the susceptibility components are complex numbers, and thus their relative phase should be considered when describing the dependence of the SHG intensity on the external magnetic field.

Using the results of the symmetry analysis performed in [16] and treating even components $\hat{\chi}^{(2),\mathrm{ev}}$ as describing quadratic in magnetization effects, the nonlinear susceptibility tensors of an isotropic metal surface and for the transversal geometry of the applied magnetic field are the following:

$$\begin{aligned}
&\chi^{\mathrm{cr}}_{xzx}=\chi^{\mathrm{cr}}_{xxz}=\chi^{\mathrm{cr}}_{yzy}=\chi^{\mathrm{cr}}_{yyz},\chi^{\mathrm{cr}}_{zxx}=\chi^{\mathrm{cr}}_{zyy},\chi^{\mathrm{cr}}_{zzz};\\
&\chi^{\mathrm{odd}}_{yxy}=\chi^{\mathrm{odd}}_{yyx},\chi^{\mathrm{odd}}_{xyy},\chi^{\mathrm{odd}}_{xxx},\chi^{\mathrm{odd}}_{xzz},\chi^{\mathrm{odd}}_{zxz}=\chi^{\mathrm{odd}}_{zzx};\\
&\chi^{\mathrm{ev}}_{xzx}=\chi^{\mathrm{ev}}_{xxz}=\chi^{\mathrm{ev}}_{yzy}=\chi^{\mathrm{ev}}_{yyz},\chi^{\mathrm{ev}}_{zxx}=\chi^{\mathrm{ev}}_{zyy},\chi^{\mathrm{ev}}_{zzz},
\end{aligned}\tag{A1}$$

where the z axis is directed along the normal to the sample's surface.

The combination of these components for a certain polarization combination determines the SHG response. Although $\chi^{i}_{\alpha\beta\gamma}$ components are complex numbers, we will assume for simplicity that they have the same phase that is independent of the angle of incidence of the pump beam. This assumption seems to be reasonable, as the fundamental and SHG radiation is far from the resonances of all the constituent materials of the samples under study. Thus we can denote the phase shifts between the $\chi^{\mathrm{odd}}_{\alpha\beta\gamma}$ and $\chi^{\mathrm{cr}}_{\alpha\beta\gamma}$ components as ϕ; ψ is the phase shift between the $\chi^{\mathrm{ev}}_{\alpha\beta\gamma}$ and $\chi^{\mathrm{cr}}_{\alpha\beta\gamma}$ components.

Below we will discuss the experiments for the p-polarized SHG excited by the linearly (p-) or circularly (c-) polarized fundamental radiation. The amplitude of the p-polarized SHG field excited by the p-polarized fundamental radiation ($E_x = E_0 \cos\theta e^{i\omega t}$, $E_y = 0$, $E_z = E_0 \sin\theta e^{i\omega t}$) in the electric dipole approximation takes the form

$$E^{pp}_{2\omega}(M) \propto \chi^{\mathrm{cr}}_{pp} + \chi^{\mathrm{odd}}_{pp} e^{i\phi} + + \chi^{\mathrm{ev}}_{pp} e^{i\psi}, \tag{A2}$$

where the *effective* nonmagnetic, linear, and quadratic in M susceptibility components are

$$\begin{aligned}
\chi^{\mathrm{cr}}_{pp} &= |\chi^{\mathrm{cr}}_{zzz}|\sin^3\theta + |\chi^{\mathrm{odd}}_{zxx}|\sin\theta\cos^2\theta + |\chi^{\mathrm{cr}}_{xxz}|\cos\theta\sin 2\theta,\\
\chi^{\mathrm{odd}}_{pp} &= |\chi^{\mathrm{odd}}_{xxx}|\cos^3\theta + |\chi^{\mathrm{odd}}_{xzz}|\cos\theta\sin^2\theta + |\chi^{\mathrm{odd}}_{zxz}|\sin\theta\sin 2\theta,\\
\chi^{\mathrm{ev}}_{pp} &= |\chi^{\mathrm{ev}}_{zzz}|\sin^3\theta + |\chi^{\mathrm{ev}}_{zxx}|\sin\theta\cos^2\theta + |\chi^{\mathrm{ev}}_{xxz}|\cos\theta\sin 2\theta,
\end{aligned}\tag{A3}$$

with θ being the angle of incidence. Here, the combination of polarizations of the SHG and fundamental beams is labeled by the subscript pp.

The expression of the SHG magnetic contrast that is commonly used as a measure of the relative magnetization-induced modulation of the SHG intensity in the geometry of the transversal Kerr effect takes the form

$$\rho_{2\omega} = \frac{I_{2\omega}(M) - I_{2\omega}(-M)}{I_{2\omega}(M) + I_{2\omega}(-M)} \propto \frac{2\chi^{\mathrm{odd}}_{pp}}{\chi^{\mathrm{cr}}_{pp}}\cos\phi, \tag{A4}$$

where we assume that $|\chi^{\mathrm{ev}}_{pp}| \ll |\chi^{\mathrm{odd}}_{pp}| \ll |\chi^{\mathrm{cr}}_{pp}|$. It is clear from Eq. (A3) that the sign of χ^{odd}_{pp} and thus of $\rho_{2\omega}$ remains unchanged for any angle of incidence of the p-polarized pump beam.

For the case of circularly polarized fundamental radiation ($E_x = E_0 \cos\theta e^{i\omega t}$, $E_y = E_0 e^{i(\omega t+\pi/2)}$, $E_z = E_0 \sin\theta e^{i\omega t}$) and for p-polarized SHG, we obtain the amplitude of the second-harmonic electric field as

$$E^{\mathrm{cp}}_{2\omega}(M) \propto \chi^{\mathrm{cr}}_{\mathrm{cp}} + \chi^{\mathrm{odd}}_{\mathrm{cp}} e^{i\phi} + \chi^{\mathrm{ev}}_{\mathrm{cp}} e^{i\psi}, \tag{A5}$$

where the subscript cp denotes the combination of circular polarization of the fundamental beam and of p-polarized SHG. The effective nonmagnetic, linear, and quadratic in **M** susceptibility components are

$$\begin{aligned}
\chi^{\mathrm{cr}}_{\mathrm{cp}} &= -|\chi^{\mathrm{cr}}_{zyy}|\sin^3\theta + |\chi^{\mathrm{cr}}_{zzz}|\sin^3\theta + |\chi^{\mathrm{cr}}_{xxz}|\cos\theta\sin 2\theta,\\
\chi^{\mathrm{odd}}_{\mathrm{cp}} &= |\chi^{\mathrm{odd}}_{xxx}|\cos^3\theta - |\chi^{\mathrm{odd}}_{xyy}|\cos\theta\\
&\quad + |\chi^{\mathrm{odd}}_{xzz}|\cos\theta\sin^2\theta + |\chi^{\mathrm{odd}}_{zxz}|\sin\theta\sin 2\theta,\\
\chi^{\mathrm{ev}}_{\mathrm{cp}} &= -|\chi^{\mathrm{ev}}_{zyy}|\sin^3\theta + |\chi^{\mathrm{ev}}_{zzz}|\sin^3\theta + |\chi^{\mathrm{ev}}_{xxz}|\cos\theta\sin 2\theta.
\end{aligned}\tag{A6}$$

Unlike the case of the linearly polarized fundamental beam, for circularly polarized pump radiation, $\chi^{\mathrm{odd}}_{\mathrm{cp}}$ and consequently $\rho_{2\omega}$ can reach zero and change their sign by increasing the angle of incidence θ, which depends on the relative values of $\chi^{\mathrm{odd}}_{xxx}$, $\chi^{\mathrm{odd}}_{xyy}$, $\chi^{\mathrm{odd}}_{xzz}$, and $\chi^{\mathrm{odd}}_{zxz}$. Importantly, when the linear (odd) in magnetization part of $E^{\mathrm{cp}}_{2\omega}(M)$ is close to zero, the term $\propto M^2$ should be predominant and should be detected more easily experimentally.

ACKNOWLEDGMENTS

This work was supported by the RFBR grants 13-02-01102-a and 12-02-00988-à and the OPTEC grant for young scientists. The research is partly supported by the grant (the agreement of August 27, 2013) 02.49.21.0003 between the Ministry of Education and Science of the Russian Federation and Lobachevsky State University of Nizhny Novgorod.

REFERENCES

1. R. Meservey, P. M. Tedrow, and P. Fulde, "Magnetic field splitting of the quasiparticle states in superconducting aluminum films," Phys. Rev. Lett. **25**, 1270–1272 (1970).
2. M. N. Baibich, J. M. Broto, A. Fert, F. N. Van Dau, F. Petroff, P. Etienne, G. Creuzet, A. Friederich, and J. Chazelas, "Giant magnetoresistance of (001)Fe/(001)Cr magnetic superlattices," Phys. Rev. Lett. **61**, 2472–2475 (1988).
3. G. Binasch, P. Grunberg, F. Saurenbach, and W. Zinn, "Enhanced magnetoresistance in layered magnetic structures with antiferromagnetic interlayer exchange," Phys. Rev. B **39**, 4828–4830 (1989).
4. J. S. Moodera, L. R. Kinder, T. M. Wong, and R. Meservey, "Large magnetoresistance at room temperature in ferromagnetic thin film tunnel junctions," Phys. Rev. Lett. **74**, 3273–3276 (1995).
5. M. Julliere, "Tunneling between ferromagnetic films," Phys. Lett. A **54**, 225–226 (1975).
6. A. Granovsky, M. Kuzmichov, J. P. Clerc, and M. Inoue, "Effective-medium theory for nonlinear magneto-optics in magnetic granular alloys: cubic nonlinearity," J. Magn. Magn. Mater. **258–259**, 103–105 (2003).
7. A. Kumar, S. Fahler, H. Schlorb, K. Leistner, and L. Schultz, "Competition between shape anisotropy and magnetoelastic anisotropy in Ni nanowires electrodeposited within alumina templates," Phys. Rev. B **73**, 064421 (2006).
8. C. Dehesa-Martinez, L. Blanco-Gutierrez, M. Velez, J. Diaz, L. M. Alvarez-Prado, and J. M. Alameda, "Magneto-optical transverse Kerr effect in multilayers," Phys. Rev B **64**, 024417 (2001).
9. T. K. Xia, P. M. Hui, and D. Stroud, "Theory of Faraday rotation in granular magnetic materials," J. Appl. Phys. **67**, 2736–2741 (1990).
10. Y. R. Shen, *The Principles of Nonlinear Optics* (Wiley, 1984).
11. O. A. Aktsipetrov, "Surface nonlinear optics and nonlinear magneto-optics at Moscow State University," J. Opt. Soc. Am. B **28**, A27–A37 (2011).
12. L. C. Sampaio, J. Hamrle, V. V. Pavlov, J. Ferre, P. Georges, A. Brun, H. Le Gall, and J. Ben Youssef, "Magnetization-induced second-harmonic generation of light by exchange-coupled magnetic layers," J. Opt. Soc. Am. B **22**, 119–127 (2005).
13. V. K. Valev, M. Gruyters, A. Kirilyuk, and T. Rasing, "Direct observation of exchange bias related uncompensated spins at the CoO/Cu interface," Phys. Rev. Lett. **96**, 067206 (2006).
14. V. K. Valev, A. Kirilyuk, F. Dalla Longa, J. T. Kohlhepp, B. Koopmans, and T. Rasing, "Observation of periodic oscillations in magnetization-induced second harmonic generation at the Mn/Co interface," Phys. Rev. B **75**, 012401 (2007).
15. L. C. Sampaio, J. Hamrle, A. Mougin, J. Ferre, F. Garcia, F. Fettar, B. Dieny, and A. Brun, "In-depth selectivity of the magnetic second-harmonic generation of light in a multilayer structure," Phys. Rev. B **70**, 104403 (2004).
16. R. P. Pan, H. D. Wei, and Y. R. Shen, "Optical second harmonic generation in magnetized surfaces," Phys. Rev. B **39**, 1229–1234 (1989).
17. K. Sato, A. Kodama, M. Miyamoto, A. V. Petukhov, K. Takanashi, S. Mitani, H. Fujimori, A. Kirilyuk, and T. Rasing, "Anisotropic magnetization-induced second harmonic generation in Fe/Au superlattices," Phys. Rev. B **64**, 184427 (2001).
18. A. A. Rzhevsky, B. B. Krichevtsov, D. E. Burgler, and C. M. Schneider, "Interfacial magnetization in exchange-coupled Fe/Cr/Fe structures investigated by second harmonic generation," Phys. Rev. B **75**, 144416 (2007).
19. P. van Gelderen, S. Crampin, T. Rasing, and J. E. Inglesfield, "Effect of interface magnetic moments and quantum-well states on magnetization-induced second-harmonic generation," Phys. Rev. B **54**, R2343 (1996).
20. V. M. Dubovik and V. V. Tugushev, "Toroid moments in electrodynamics and solid-state physics," Phys. Rep. **187**, 145–202 (1990).
21. A. A. Gorbatsevich and Y. V. Kopaev, "Toroidal order in crystals," Ferroelectrics **161**, 321–334 (1994).
22. B. B. Van Aken, J. P. Rivera, H. Schmid, and M. Fiebig, "Observation of ferrotoroidic domains," Nature **449**, 702–705 (2007).
23. N. A. Spaldin, M. Fiebig, and M. Mostovoy, "The toroidal moment in condensed-matter physics and its relation to the magnetoelectric effect," J. Phys. Condens. Matter **20**, 434203 (2008).
24. O. G. Udalov, M. V. Sapozhnikov, E. A. Karashtin, B. A. Gribkov, S. A. Gusev, E. V. Skorohodov, V. V. Rogov, A. Y. Klimov, and A. A. Fraerman, "Nonreciprocal light diffraction by a lattice of magnetic vortices," Phys. Rev. B **86**, 094416 (2012).
25. V. L. Krutyanskiy, I. A. Kolmychek, B. A. Gribkov, E. A. Karashtin, E. V. Skorohodov, and T. V. Murzina, "Second harmonic generation in magnetic nanoparticles with vortex magnetic state," Phys. Rev. B **88**, 094424 (2013).
26. A. Bonda, S. Uba, and L. Uba, "Nonlinear magnetization-induced terms in garnet film polarization in the second-harmonic generation effect: theory and experiment," Phys. Rev. B **87**, 024426 (2013).
27. N. Bloembergen and P. S. Pershan, "Light waves at the boundary of nonlinear media," Phys. Rev. **128**, 606–622 (1962).
28. A. B. Granovsky, Y. Sukhorukov, E. Gan'shina, and A. Telegin, "Magnetorefractive effect in magnetoresistive materials," in *Magnetophotonics: From Theory to Applications*, M. Inoue, M. Levy, and A. V. Baryshev, eds., Vol. **178** of Springer Series in Materials Science (Springer, 2013), pp. 107–133.
29. K. H. Bennemann, "Theory for nonlinear magnetooptics in metals," J. Magn. Magn. Mater. **200**, 679–705 (1999).
30. A. K. Zvezdin and V. A. Kotov, *Modern Magnetooptics and Magnetooptical Materials* (CRC Press, 1997).
31. L. D. Landau and E. M. Lifshitz, *Electrodynamics of Continuous Media*, Vol. **8** of Course of Theoretical Physics (Butterworth-Heinemann, 1984).
32. V. L. Ginzburg, *The Propagation of Electromagnetic Waves in Plasmas* (Gordon and Breach, 1962).
33. A. L. Shelankov and G. E. Pikus, "Reciprocity in reflection and transmission of light," Phys. Rev. B **46**, 3326–3336 (1992).
34. A. Barone and G. Paterno, *Physics and Applications of the Josephson Effect* (Wiley, 1982).
35. O. A. Aktsipetrov, T. V. Murzina, E. M. Kim, R. V. Kapra, A. A. Fedyanin, M. Inoue, A. F. Kravets, S. V. Kuznetsova, M. V. Ivanchenko, and V. G. Lifshits, "Magnetization-induced second- and third-harmonic generation in magnetic thin films and nanoparticles," J. Opt. Soc. Am. B **22**, 138–147 (2005).
36. A. Kirilyuk, "Nonlinear optics in application to magnetic surfaces and thin films," J. Phys. D **35**, R189–R207 (2002).
37. I. A. Kolmychek and T. V. Murzina, "Magnetization-induced anisotropy of second harmonic generation in thin cobalt films," J. Magn. Magn. Mater. **323**, 2973–2976 (2011).